Inhibiting MAPK14 showed anti-prolactinomas effect

Qiaoyan Ding
The third hospital of Wuhan
Yu Zhang
Hubei University of Chinese Medicine
Li Ma
The third hospital of Wuhan
Yong-gang Chen
The third hospital of Wuhan
Jin-hu Wu
The third hospital of Wuhan
Hong-feng Zhang
The central hospital of Wuhan
Xiong Wang (wangxiong-133494@163.com)

Research article

Keywords: Prolactinomas, Prolactin, MAPK14, DRD2

Posted Date: May 1st, 2020

DOI: https://doi.org/10.21203/rs.3.rs-22129/v1

Version of Record: A version of this preprint was published on September 7th, 2020. See the published version at https://doi.org/10.1186/s12902-020-00619-z.

Abstract

Background The pathogenesis of prolactinomas has not been clarified yet. p38 MAPK signaling including p38α MAPK (MAPK14), p38β (MAPK11), p38γ (MAPK12) and p38δ (MAPK13) is related to the development and progression of many cancers. We sought to investigate the role of MAPK14 in prolactinomas.

Methods Immunofluorescence assay was performed on the prolactin (PRL) and MAPK14 protein expressions of pituitary gland in C57BL/6 mice and human prolactinomas specimens. We analyzed the role of MAPK14 in prolactinomas using estradiol-induced model and $DRD2^{-/-}$ model in C57BL/6 wild-type (WT), $MAPK14^{-/-}$, $DRD2^{-/-}MAPK14^{+/-}$ mice. GH3 cells were transfected with different sets of MAPK14 siRNA, which to study MAPK14 and PRL protein expression in GH3.

Results Immunofluorescenc assaye found that PRL and MAPK14 were co-locatied and increased significantly in the pituitary gland of estradiol-injected prolactinomas mice than in control mice. And the deficiency of MAPK14 significantly inhibited the tumor overgrowth, along with the PRL decrease in estradiol-induced mice. Furthermore, MAPK14 deficiency in $DRD2^{-/-}MAPK14^{+/-}$ mice significantly inhibited the overgrowth of pituitary gland and PRL production and secretion than in $DRD2^{-/-}$ mice. And MAPK14 knockdown by siRNA inhibited PRL production in GH3 cells.

Conclusion The results establish that MAPK14 plays a promoting role in the formation of prolactinomas, and validate MAPK14 as potential therapeutic target.

1. Background

As a kind of intracranial tumors, pituitary tumor seriously damage human health. The morbidity of pituitary tumor is 5/100,000, in which 50% is prolactinomas [1,2]. The tumor cells of prolactinomas secrete excess of prolactin, resulting in many symptoms such as sterility, hyperprolactinemia, amenorrhea, galactorrhea, pituitary space occupying lesion [3]. The cause of prolactinomas is unclear yet, perhaps due to hypothalamic disorder or inherent defect of pituitary cells. A present, dopamine agonist bromocriptine which binds to dopamine D2 receptors (D2R), is regarded as the first-line therapies for treating prolactinomas [1]. However, nearly 10% of prolactinomas patients do not respond to bromocriptine [4]. This tumor represents a major challenge for clinical management. Therefore, it is urgent to clarify the pathogenesis and develop new medical treatments for prolactinomas. MAPK is an important transmitter of signal from cell surface to nucleus, which includes extracellular signal-regulated kinase (ERK1/2), p38 MAPK and c-jun-Nterminal kinase (JNK1/2) [5]. The p38 MAPK related proteins p38α (MAPK14), p38β (MAPK11), p38γ (MAPK12), and p38δ (MAPK13) share very similar protein sequences, which are activated by dual phosphorylation mediated primarily by the MAPK kinases (MKK)3 and MKK6 in response to a range of cell stresses and to inflammatory cytokines [6]. MAPK14 is the most abundant, best-characterized isoform, which participates in the process of many physiological activities and diseases. In recently years, many scientists reported that MAPK14 played a cruial role in the

inflammatory response in vivo using gene knockout mice [7-9]. And more, MAPK14 inhibitor has been confirmed in animal experiment and used to treat colitis in clinical trials [10-13].

These findings suggest that MAPK14 palys a important role in the formation and development of prolactinomas. According to the literature report[14] and previous experience, the model of estradiol-induced prolactinoma in mice was established. Cristina[15] and Seruggia[16] confirmed that DRD2 knockout can produce a stable and reliable prolactinoma mice model (C57BL/6), so C57BL/6 WT mice were used as the control. In order to make the results more credible, we also used the prolactinoma model of $DRD2^{-/-}$ mice. Here, the estradiol-induced model and $DRD2^{-/-}$ model were used to study prolactinomas development in control/WT mice and in mice lacking MAPK14. We hypothesised that blockade of MAPK14 expression in the mice largely suppressed tumor formation of pituitary gland and PRL production and secretion in estradiol-induced and $DRD2^{-/-}$ prolactinomas. This illustrates the critical prooncogenic role of MAPK14 for prolactinomas, and MAPK14 was expected to be potential target for prolactinomas treatment.

2. Methods

2.1. Animals

Female C57BL/6 mice (weighing 20±5 g) were purchase from Hubei Experimental Animal Center (Wuhan, PR China). $DRD2^{-/-}$ and $MAPK14^{-/-}$ mice were described previously [17,18]. $DRD2^{-/-}$ and $MAPK14^{-/-}$ mice were hybridized to breed $DRD2^{-/-}MAPK14^{+/-}$ mice. All animal experiments were approved by the Ethics Committee of Tongren hospital affiliated to Wuhan University (The third hospital of Wuhan). All the mice were housed and bred in specific pathogen-free (SPF) grade cages and provided with autoclaved food and water.

2.2. Human pituitary gland specimens

Pituitary gland samples were collected from 27 prolactinomas patients and 21 other pituitary disease patients after surgical excision (the central hospital of Wuhan, Tongji medical college, Huazhong University of Science and Technology). All samples and datas of participants were deidentified. This study was approved by the Institutional Research Ethics Committee of the central hospital of Wuhan, Tongji medical college, Huazhong University of Science and Technology.

2.3. Animal models and grouping

On the one hand, the mice were randomly assigned to control/WT (n = 9), Estradiol benzoate (ES) (n = 9) and $MAPK14^{-/-}$ ES (n = 6). ES was injected into the abdominal cavity of mice according to the dosage of 20 $mg{\cdot}kg^{-1}$ every time and was carried out once every 4 days and lasted for 32 days. The prolactinomas mice model was successfully established. On the other hand, the mice were randomly assigned to WT (n = 6), $DRD2^{-/-}$ (n = 6) and $DRD2^{-/-}$ $MAPK14^{+/-}$ ES (n = 6). At the age of 8 months, the pituitary gland of $DRD2^{-/-}$ mice proliferates and prolactinomas forms, which is the model mouse of prolactinomas [15].

2.4. Sample collection

After successful modeling, all mice were anesthetized with an intraperitoneal injection of 1% pentobarbital sodium. Then, blood samples were drawn from the abdominal aorta, transferred into dried tubes containing EDTA as an anticoagulant, and centrifuged at 2400 rpm for 15 min. The upper serum is collected in a clean centrifuge tube and stored at 4℃. The pituitary gland was removed after the mice were sacrificed by cervical dislocation. The pituitary gland used for immunofluore- scence experiment was stored in formalin solution at room temperature. The pituitary gland used in other experiments was placed in a cryopreserved tube and stored at -80℃. The dead mice were sent to the laboratory animal treatment center of the hospital for unified treatment.

2.5. Immunofluorescence assay

Tissue specimens of pituitary gland were routinely formalin-fixed, paraffin- embedded and sectioned into 5 μm pieces for immunofluorescence. Paraffin sections were dewaxed to water, and tissue sections were placed filled with EDTA antigen repair buffer (pH 8.0) for antigen repair. After natural cooling, the sections were washed in PBS (pH 7.4) for 3 times. After the sections were slightly dried, a histochemical pen was used to draw a circle around the tissue, and the autofluorescence quenching agent was added into the circle for 5 min, and the sections were rinsed with flowing water for 10 min, then BSA was added into the circle to incubate for 30 min. Primary antibody MAPK14 (1: 1000, Proteintech), PRL (1: 1000, R&D Systems) were added into the sections and incubated overnight at 4℃. The sections were washed with PBS for 3 times and incubated with secondary antibody at room temperature for 50 min. Then the sections were washed with PBS for 3 times and sealed with anti-fluorescence quenching tablet. The sections were observed under the fluorescence microscope.

2.6. ELISA test

The expression levels of PRL in mice serum were detected in strict accordance with the provided instructions of ELISA kits: PRL (E-EL-M0083c) (Elabscience, Wuhan, China). Firstly, 100 μL standard working fluid or sample were added to the corresponding plate hole and incubate for 37 min. After discarding the liquid in the plate, 100 μL biotinylated antibody working fluid was immediately added to the plate hole and incubated for 60 min at 37℃. Discard the liquid in the board and wash the board 3 times. Secondly, 100 μL HRP enzyme conjugate working fluid was added to each plate hole and incubated for 30 min at 37℃, discard the liquid in the plate, and wash the plate for 5 times. Then, 90 μL of substrate solution was added to each plate hole and incubated for about 15 minutes at 37℃. Finally, 50 μL termination fluid was added to each plate hole to terminate the reaction. Optical density value of each sample was measured within 3 min using a microplate reader (Molecular Devices) at a wavelength of 450 nm.

2.7. Real-Time PCR(RT-qPCR) analysis

Total RNA from cells or tissue was extracted using the RNA extraction kit (TIANGEN, Beijing, China). cDNA was synthesized using the RNA PCR Kit (Thermo Fisher Scientific, Waltham, MA, USA). The thermocycling conditions for RT-qPCR were: 95℃ for 10 min, followed by 40 cycles of 95℃ for 30 sec , 55℃ for 1 min and 72℃ for 30 sec, at last is 95℃ for 1 min and 55℃ for 30 sec. PCR was carried out using the FastStart Universal SYBR Green Master Mix (Roche Diagnostics, Mannheim, Germany) on an Mx3000P Real-Time PCR system (Agilent Technologies Stratagene, USA). The sequences of the primers were: Actin forward, GTGCTATGTTGCTCTAGACTTCG; and reverse, ATGCCACAGGATTCCATACC; PRL forward, TCAGCCCAGAAAGGGACACTCC; and reverse, CAGCGGAACA- GATTGGCAGAGG.

2.8. Cell culture

GH3 cell lines were purchased from BeNa Culture Collection (BNCC) Cell Bank (Beijing, China) and were cultured in DMEM (Gibco, Thermo Fisher Scientific, China) supplemented with 1% FBS (SeraPro, South America) at 37℃ under 5% CO2.

2.9. RNA interference

Three diffffferent sets of siRNA sequences for MAPK14 were designed and synthesised by Guangzhou Ribobio Co.,LTD (Guangzhou, China). Three siRNA sequences for MAPK14 were as follows: 1) GGTCCCTGGAGGAATTCAA; 2) CCGAAGATGAACTTCGCAA; 3) GGACCTCCTT- ATAGACGAA. GH3 cells were seeded into a 6-well plate at a density of 200,000 cells/well and transfected with diffffferent sets of MAPK14 siRNA in each well respectively. The cells were transfected using Lipofectamine2000 (Invitrogen) according to the manufacturer's instructions.

2.10. Western blot

Pituitary glands were obtained and stored at -80℃. The samples were put into some lysis buffer with protease inhibitors to prepare the tissue protein in the homogenizing tubes, then they were blended with a tissue homogenizer(Wuhan Servicebio). The protein concentration of samples were determined using the Bradford protein assay. 10 or 12% SDS-PAGE gels were used to separate the protein samples, which then were transferred to nitrocellulose membranes. At last, the membranes were blocked by 5% of milk proteins and then incubated with primary antibodies at 4℃ overnight. THE antibodies were as follows: Rabbit anti-mice PRL (Affinity Biosciences), rabbit anti-mice MAPK14 (Proteintech Group Inc.), and mouse anti-β-actin (Abclonal Biotech Co.). Blots were washed for three times, and then incubated with secondary horseradish peroxidase-conjugated antibodies, and detected using ECL Western blotting detection reagents (Shanghai Jiapeng). All protein expression of samples was quantified using the Fluor-S-Multi Imager (Shanghai Jiapeng) and Quantity One 4.2.1 software. The band intensity was normalized to the β-actin band.

2.11. Statistical analysis

All data were expressed as mean ± S.E.M. Graphpad prism 8.0 software was used for all statistical analysis and graph production. One-way analysis of variance was used to compare the differences

among groups. Values of $P < 0.05$ were considered statistically significant.

3. Results

3.1. The health status of mice

All mice had no abnormality, normal diet and drinking water, and no death. There was no significant change in the body weight of the mice, which ranged from 15 to 25 g.

3.2. PRL and MAPK14 were overexpressed and co-locatied in the pituitary gland of estradiol-injected prolactinomas mice and human prolactinomas specimens

Immunofluorescence assay was performed on the PRL and MAPK14 protein expressions of pituitary gland in mice and human prolactinomas specimens. The result showed that PRL and MAPK14 were overexpressed and co-locatied in the pituitary gland of estradiol-injected prolactinomas mice(Fig.1A, B and C) and human prolac- tinomas specimens (Fig.1D, E and F). Compared with control mice, the PRL and MAPK14 expression of pituitary gland in prolactinomas mice increased significantly (Fig.1B and C, $P<0.05$). And compared with human PRL negative specimens, the PRL and MAPK14 expresson of pituitary gland in human prolactinomas specimens increased significantly too (Fig.1E and F, $P<0.001$).

3.3. MAPK14 knockout inhibited the overgrowth of pituitary gland and PRL production and secretion in estradiol-injected prolactinoma mice

Compared with the WT mice, the serum PRL level of peripheral blood by ELISA (Fig.2A, $P<0.01$) and PRL mRNA level of pituitary gland by RT-qPCR (Fig.2B, $P<0.01$) increased, and pituitary gland weight/body weight (Fig.2C, $P<0.001$) increased significantly in estradiol-injected mice. Compared with the estradiol-injected mice, the serum PRL level of peripheral blood by ELISA (Fig.2A, $P<0.01$) and PRL mRNA level of pituitary gland by RT-qPCR (Fig.2B, $P<0.05$) decreased, and tumor/body weight (Fig.2C, $P<0.001$) decreased significantly in estradiol-injected MAPK14$^{-/-}$ mice. Western blot result showed that compare with the wild type mice, PRL protein of pituitary gland increased significantly in estradiol-injected mice ($P<0.01$), which was reversed in estradiol-injected MAPK14$^{-/-}$ mice ($P<0.05$) (Fig.2D and E).

3.4. MAPK14 half-knockout inhibited the overgrowth of pituitary gland and PRL production and secretion in DRD2$^{-/-}$ mice

Compared with the WT mice, the serum PRL level of peripheral blood by ELISA (Fig.3A, $P<0.01$) and PRL mRNA level of pituitary gland by RT-qPCR (Fig.3B, $P<0.01$) increased, and pituitary gland weight/body weight (Fig.3C, $P<0.001$) increased significantly in DRD2$^{-/-}$ mice. Compared with the DRD2$^{-/-}$ mice, the serum PRL level of peripheral blood by ELISA (Fig.3A, $P<0.01$) and PRL mRNA level of pituitary gland by RT-qPCR (Fig.3B, $P<0.05$) decreased, and tumor/body weight (Fig.3C, $P<0.001$) decreased significantly in DRD2$^{-/-}$MAPK14$^{+/-}$ mice. Western blot result showed that compare with the wild type mice, PRL protein of

pituitary gland increased significantly in DRD2$^{-/-}$ mice (P<0.01), which was reversed in DRD2$^{-/-}$MAPK14$^{+/-}$ mice (P<0.05) (Fig.3D, E and F).

3.5. MAPK14 knockdown by siRNA inhibited PRL production in GH3 cells

GH3 cells were transfected with different sets of MAPK14 siRNA. Then RT-qPCR was used to determine the mRNA levels of MAPK14 and PRL, and protein expressions were determined by western blot. Compared with the negative control (NC) group, transfection of MAPK14 siRNA (30 nM, 50 nM, 100 nM) signifcantly decreased the expression of MAPK14 in GH3 cells in a dose-dependent manner (Fig.4A, C and D), which resulting in the PRL expression decrease signifcantly in a dose-dependent manner (Fig.4B, C and E).

4. Discussion

Most of prolactinomas patients appear drug response to dopamine agonist bromocriptine, including the reduction of tumor size and the decrease of PRL production and secretion [19]. Bromocriptine which acts on DRD2 is regarded as the first-line therapies for treating prolactinomas. However, 10 % of prolactinomas patients show severe drug resistance even at high doses of bromocriptine, and the resistant mechanism has not been clarified yet [20]. This phenomenon bring a major challenge for clinical treatment. Therefore, it is urgent to explore the pathogenesis of prolactinomas and develop new therapeutic targets.

The MAPK pathway is related to various kinds of cancer [21]. There have been many reports that p38 MAPK participated in the development of liver cancer [22], breast cancer [23,24], lung cancer [25], bladder cancer [26,27], prostate cancer [28-30], leukemia [31] and transformed follicular lymphoma [32,33]. However, the relevance of the MAPK14 pathway with prolactinomas has not been reported yet. In order to further study the pathogenesis of human prolactin adenoma and develop corresponding therapeutic drugs, it is feasible to establish an animal model similar to it. At present, estradiol-injected and DRD2 knockout mice were most frequent animal model used to study the prolactinomas. The estradiol-injected model established in our study was successful and easily performed, along with high stability. Although the DRD2 knockout model we established is time-consuming, it is more beneficial to the research at the molecular level.

Here, we found that PRL and MAPK14 proteins were co-locatied and expressed more significantly in the pituitary gland of estradiol-injected prolactinomas mice than in control mice. The same results were obtained in human prolactinomas specimens. Furthermore, we found that the deficiency of MAPK14 significantly decreased tumor size, along with the decrease of PRL production and secretion in estradiol-injected prolactinomas mice and DRD2$^{-/-}$ mice, confirming that MAPK14 promotes the formation of prolactinomas.

Our current findings demonstrates that role of MAPK14 in promoting the overgrowth of pituitary gland and PRL production and secretion. Given the function of MAPK14 in the progression of prolactinomas,

MAPK14 could be further explored to be a novel clinical therapeutic target for prolactinomas.

5. Conclusion

This was the first study to demonstrate that inhibition of MAPPK14 can inhibit the growth of prolactinomas, and the production and secretion of PRL. This confirms that inhibition of MAPK14 showed anti-prolactinoma effects.

Abbreviations

PRL:Prolactin; MAPK:Mitogen-activated protein kinase; DRD2:Dopamine D2 receptor; siRNA:Small interfering RNA; ELISA:Enzyme-Linked Immuno sorbent Assay; ES:Estradiol benzoate; WT:Wild type.

Declarations

Ethics approval and consent to participate

All animal experiments were approved by the Ethics Committee of Tongren hospital affiliated to Wuhan University (the third hospital of Wuhan). All samples and datas of participants were deidentified. This study was approved by the Institutional Research Ethics Committee of the central hospital of Wuhan, Tongji medical college, Huazhong University of Science and Technology. This study was conducted in accordance with the Guide for the Care and Use of Laboratory Animals (NIH Publication NO.85-23, revised 1996). All applicable international, national, and/or institutional guidelines for the care and use of animals were followed.

Consent for publication

Not applicable

Availability of data and materials

All data generated or analyzed during this study and supporting our findings are included and can be found in the manuscript. The raw data can be provided by corresponding author on reasonable request.

Competing interests

The authors declare no conflict of interest.

Funding

This work was supported by the Natural Science Foundation of China (No. 81603352), Hubei Natural Science Foundation (2017CFB125), and Scientific Research Project Funds for Wuhan Health and Family Planning Commission (WZ16A10). The funders had no role on the study design, data analysis, interpretation and writing the manuscript in this study.

Authors' contributions

QD performed the majority of experiments and drafted the paper. YZ, LM, JW and YC helped with experiments and analyzed the data. XW and HZ conceived the study, supervised the experiments and edited the manuscript. All authors read and approved the final manuscript.

Acknowledgments

We thank Dr. Rongbin Zhou (Chinese University of Science and Technology) for providing DRD2$^{-/-}$ mice, and Dr. Jiahuai Han (Xiamen University) for providing MAPK14$^{-/-}$ mice.

References

[1] Colao A and Savastano S: Medical treatment of prolactinomas. Nat Rev Endocrinol. 2001;7:267–278.

[2] Daly AF, Rixhon M, Adam C, Dempegioti A, Tichomirowa MA and Beckers A: High prevalence of pituitary adenomas: a cross-sectional study in the province of Liege, Belgium. J Clin Endocrinol Metab. 2006;91:4769–4775.

[3] Gillam MP, Molitch ME, Lombardi G and Colao A: Advances in the treatment of prolactinomas. Endocr Rev. 2006;27:485–534.

[4] Oh MC and Aghi MK: Dopamine agonist-resistant prolactinomas. J Neurosurg. 2011;114:1369-1379.

[5] Cuenda A and Rousseau S: p38 MAP-kinases pathway regulation, function and role in human diseases. Biochim Biophys Acta. 2007;1773:1358–1375.

[6] Remy G, Risco AM, Iñesta-Vaquera FA, González-Terán B, Sabio G, Davis RJ and Cuenda A: Differential activation of p38MAPK isoforms by MKK6 and MKK3. Cell Signal. 2010;22:660–667.

[7] Kang YJ, Chen J, Otsuka M, Mols J, Ren S, Wang Y and Han J: Macrophage deletion of p38alpha partially impairs lipopolysaccharide-induced cellular activation. J Immunol. 2008;180:5075–5082.

[8] Kim C, Sano Y, Todorova K, Carlson BA, Arpa L, Celada A, Lawrence T, Otsu K, Brissette JL, Arthur JS, et al: The kinase p38 alpha serves cell type-specific inflammatory functions in skin injury and coordinates proand anti-inflammatory gene expression. Nat Immunol. 2008; 9:1019–1027.

[9] Otsuka M, Kang YJ, Ren J, Jiang H, Wang Y, Omata M and Han J: Distinct effects of p38alpha deletion in myeloid lineage and gut epithelia in mouse models of inflammatory bowel disease. Gastroenterology. 2010;138:1255–1265.

[10] Hommes D, van den Blink B, Plasse T, Bartelsman J, Xu C, Macpherson B, Tytgat G, Peppelenbosch M and Van Deventer S: Inhibition of stress-activated MAP kinases induces clinical improvement in moderate to severe Crohn's disease. Gastroenterology. 2002;122:7–14.

[11] Hollenbach E, Neumann M, Vieth M, Roessner A, Malfertheiner P and Naumann M: Inhibition of p38 MAP kinase- and RICK/NF-kappaB-signaling suppresses inflammatory bowel disease. FASEB J. 2004;18:1550–1552.

[12] Schreiber S, Feagan B, D'Haens G, Colombel JF, Geboes K, Yurcov M, Isakov V, Golovenko O, Bernstein CN, Ludwig D, et al: Oral p38 mitogen-activated protein kinase inhibition with BIRB 796 for active Crohn's disease: a randomized, double-blind, placebo-controlled trial. Clin Gastroenterol Hepatol. 2006;4:325–334.

[13] ten Hove T, van den Blink B, Pronk I, Drillenburg P, Peppelenbosch MP and van Deventer SJ: Dichotomal role of inhibition of p38 MAPK with SB 203580 in experimental colitis. Gut. 2002;50:507–512.

[14] Heaney AP, Horwitz GA, Wang Z, Singson R and Melmed S: Early involvement of estrogen-induced pituitary tumor transforming gene and fibroblast growth factor expression in prolactinoma pathogenesis. Nat Med. 1999;5:1317-1721.

[15] Cristina C, García-Tornadú I, Díaz-Torga G, Rubinstein M, Low MJ, Becú- Villalobos D: Dopaminergic D2 receptor knockout mouse: an animal model of prolactinoma. Front Horm Res. 2006;35:50-63.

[16] Seruggia D, Montoliu L:The new CRISPR-Cas system: RNA-guided genome engineering to efficiently produce any desired genetic alteration in animals. Transgenic Res. 2014;23:707-716.

[17] Kelly MA, Rubinstein M, Asa SL, Zhang G, Saez C, Bunzow JR, Allen RG, Hnasko R, Ben-Jonathan N, Grandy DK, et al: Pituitary lactotroph hyperplasia and chronic hyperprolactinemia in dopamine D2 receptor-deficient mice. Neuron. 1997;19: 103-113.

[18] Otsuka M, Kang YJ, Ren J, Jiang H, Wang Y, Omata M and Han J: Distinct effects of p38alpha deletion in myeloid lineage and gut epithelia in mouse models of inflammatory bowel disease. Gastroenterology. 2010;138:1255-1265.

[19] Wong A, Eloy JA, Couldwell WT and Liu JK. Update on prolactinomas. Part 2: Treatment and management strategies. J Clin Neurosci. 2015;22:1568-1574.

[20] Vroonen L, Jaffrain-Rea ML, Petrossians P, Tamagno G, Chanson P, Vilar L, Borson-Chazot F, Naves LA, Brue T, Gatta B, et al: Prolactinomas resistant to standard doses of cabergoline: a multicenter study of 92 patients. Eur J Endocrinol. 2012;167:651-662.

[21] Burotto M, Chiou VL, Lee JM and Kohn EC: The MAPK pathway across different malignancies: A new perspective. Cancer. 2014;120:3446–3456.

[22] Iyoda K, Sasaki Y, Horimoto M, Toyama T, Yakushijin T, Sakakibara M, Takehara T, Fujimoto J, Hori M, Wands JR, et al: Involvement of the p38 mitogen-activated protein kinase cascade in hepatocellular carcinoma. Cancer.2003; 97:3017-3026.

[23] Tsai PW, Shiah SG, Lin MT, Wu CW and Kuo ML: Up-regulation of vascular endothelial growth factor C in breast cancer cells by heregulin-beta 1. A critical role of p38/nuclear factor-kappa B signaling pathway. J Biol Chem. 2003;278:5750-5959.

[24] Suarez-Cuervo C, Merrell MA, Watson L, Harris KW, Rosenthal EL, Väänänen HK and Selander KS: Breast cancer cells with inhibition of p38alpha have decreased MMP-9 activity and exhibit decreased bone metastasis in mice. Clin Exp Metastasis. 2004;21:525-533.

[25] Greenberg AK, Basu S, Hu J, Yie TA, Tchou-Wong KM, Rom WN and Lee TC: Selective p38 activation in human non-small cell lung cancer. Am J Respir Cell Mol Biol. 2002;26:558-564.

[26] Kumar B, Sinclair J, Khandrika L, Koul S, Wilson S and Koul HK: Differential effects of MAPKs signaling on the growth of invasive bladder cancer cells. Int J Oncol. 2009;34:1557-1564.

[27] Kumar B, Koul S, Petersen J, Khandrika L, Hwa JS, Meacham RB, Wilson S and Koul HK: p38 mitogenactivated protein kinase-driven MAPKAPK2 regulates invasion of bladder cancer by modulation of MMP-2 and MMP-9 activity. Cancer Res. 2010;70:832-841.

[28] Park JI, Lee MG, Cho K, Park BJ, Chae KS, Byun DS, Ryu BK, Park YK and Chi SG: Transforming growth factor-beta1 activates interleukin-6 expression in prostate cancer cells through the synergistic collaboration of the Smad2, p38-NF-kappaB, JNK, and Ras signaling pathways. Oncogene. 2003;22:4314-4332.

[29] Khandrika L, Lieberman R, Koul S, Kumar B, Maroni P, Chandhoke R, Meacham RB and Koul HK: Hypoxia-associated p38 mitogen-activated protein kinase-mediated androgen receptor activation and increased HIF-1alpha levels contribute to emergence of an aggressive phenotype in prostate cancer. Oncogene. 2009;28:1248-1260.

[30] Maroni PD, Koul S, Meacham RB and Koul HK: Mitogen activated protein kinase signal transduction pathways in the prostate. Cell Commun Signal. 2004;2: 5.

[31] Liu RY, Fan C, Liu G, Olashaw NE and Zuckerman KS: Activation of p38 mitogen-activated protein kinase is required for tumor necrosis factor-alpha-supported proliferation of leukemia and lymphoma cell lines. J Biol Chem. 2000;275:21086- 21093.

[32] Elenitoba-Johnson KS, Jenson SD, Abbott RT, Palais RA, Bohling SD, Lin Z, Tripp S, Shami PJ, Wang LY, Coupland RW, et al: Involvement of multiple signaling pathways in follicular lymphoma transformation: p38-mitogen-activated protein kinase as a target for therapy. Proc Natl Acad Sci U S A. 2003;100:7259-7264.

[33] Lin Z, Crockett DK, Jenson SD, Lim MS and Elenitoba-Johnson KS: Quantitative proteomic and transcriptional analysis of the response to the p38 mitogen-activated protein kinase inhibitor SB203580 in transformed follicular lymphoma cells. Mol Cell Proteomics. 2004;3:820-833.

Figures

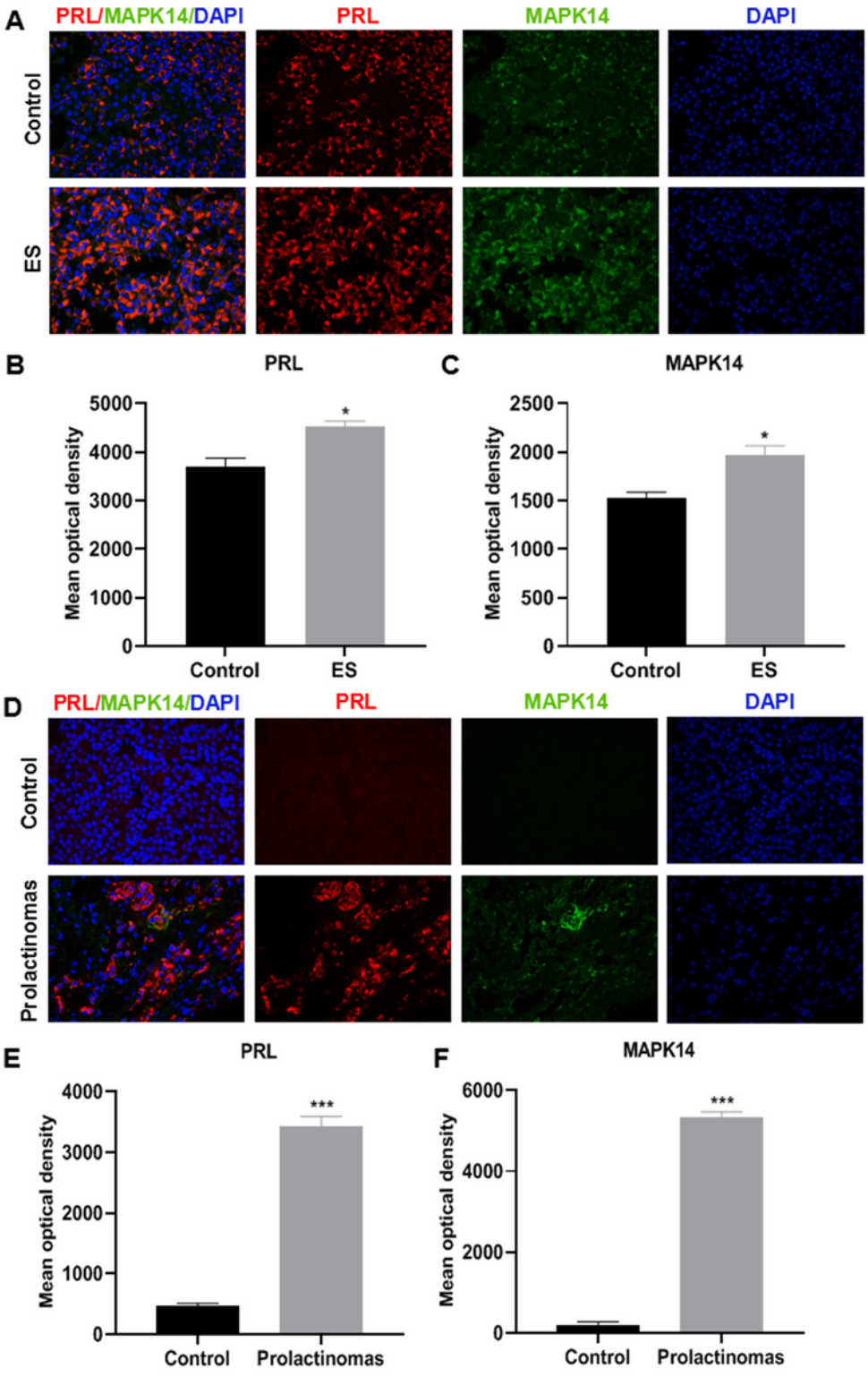

Figure 1

Immunofluorescence assay of PRL and MAPK14 protein expressions. (magnification × 400). (A) The PRL and MAPK14 Immunofluorescence expression of pituitary gland in control mice and prolactinomas mice. (B, C) Mean optical density value of PRL and MAPK14 protein expressions were quantitatively examined

by image analysis system. *P<0.05 compared with Control group, (n = 4). (D) The PRL and MAPK14 Immunofluore- scence expression of pituitary gland in human PRL negative specimens and human prolactinomas specimens. (E, F) Mean optical density value of PRL and MAPK14 protein expressions were quantitatively examined by image analysis system. ***P<0.001 compared with Control group, (n = 4). Red: PRL, Green: MAPK14, Blue: DAPI.

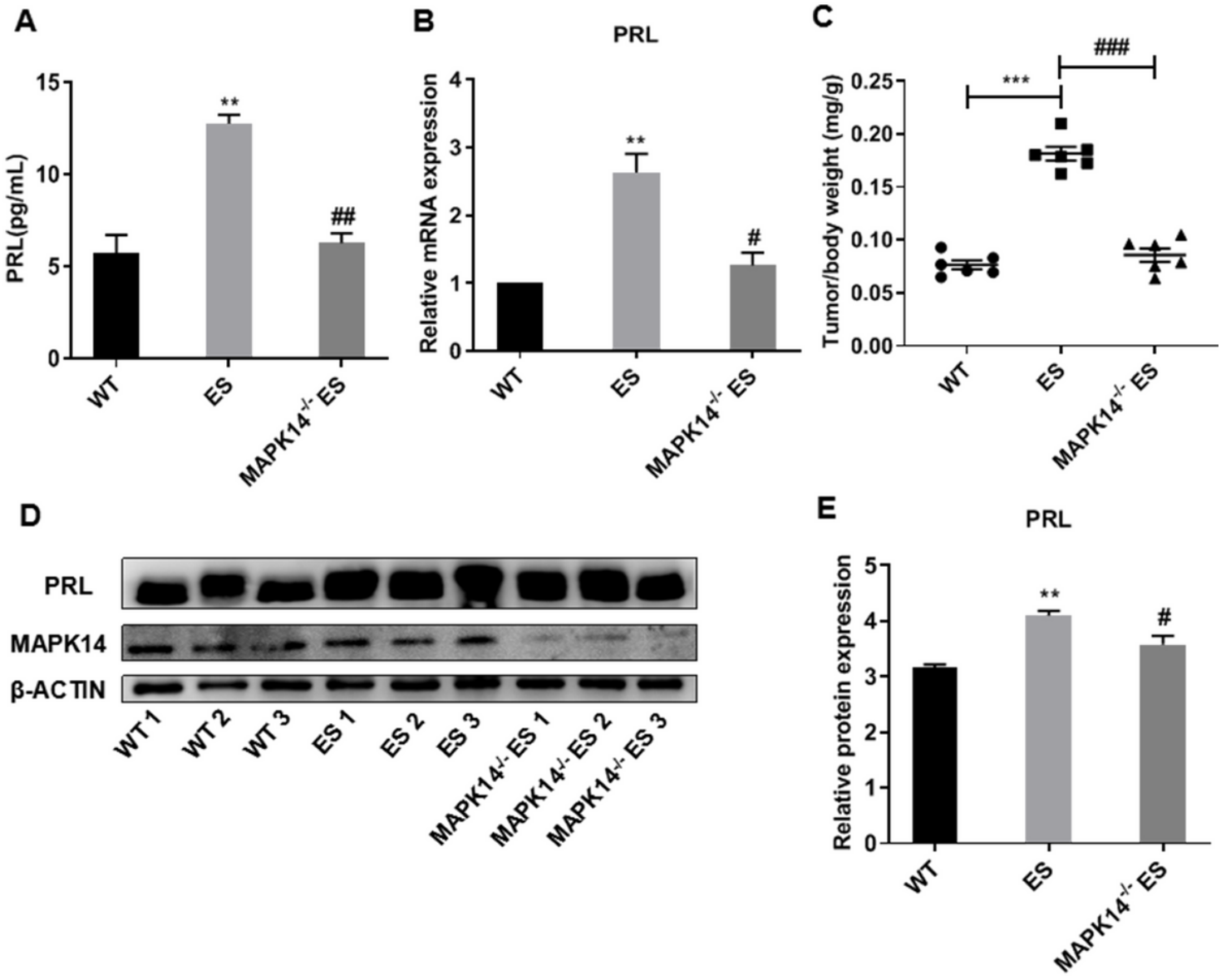

Figure 2

Effects of MAPK14 knockout on the development of prolactinomas in estradiol-induce mice. (A) Serum PRL level of wild-type (WT) mice, ES-injected mice and ES-injected MAPK14-/- mice by ELISA. **P<0.01 compared with WT group, ##P<0.01 compared with ES group, (n = 3). (B) The relative PRL mRNA expressions of pituitary gland in mice were detected by RT-qPCR. **P<0.01 compared with WT group, ##P<0.01 compared with ES group, (n = 3). (C) The pituitary gland weight/body weight was calculated. ***P<0.001 compared with WT, ###P<0.001 compared with ES group, (n = 6). (D) The PRL protein expressions of pituitary gland in mice were detected by western blot. (E) The relative PRL protein

expression was quantifed via normalization to β-actin. **P<0.01 compared with WT group, #P<0.05 compared with ES group, (n = 3).

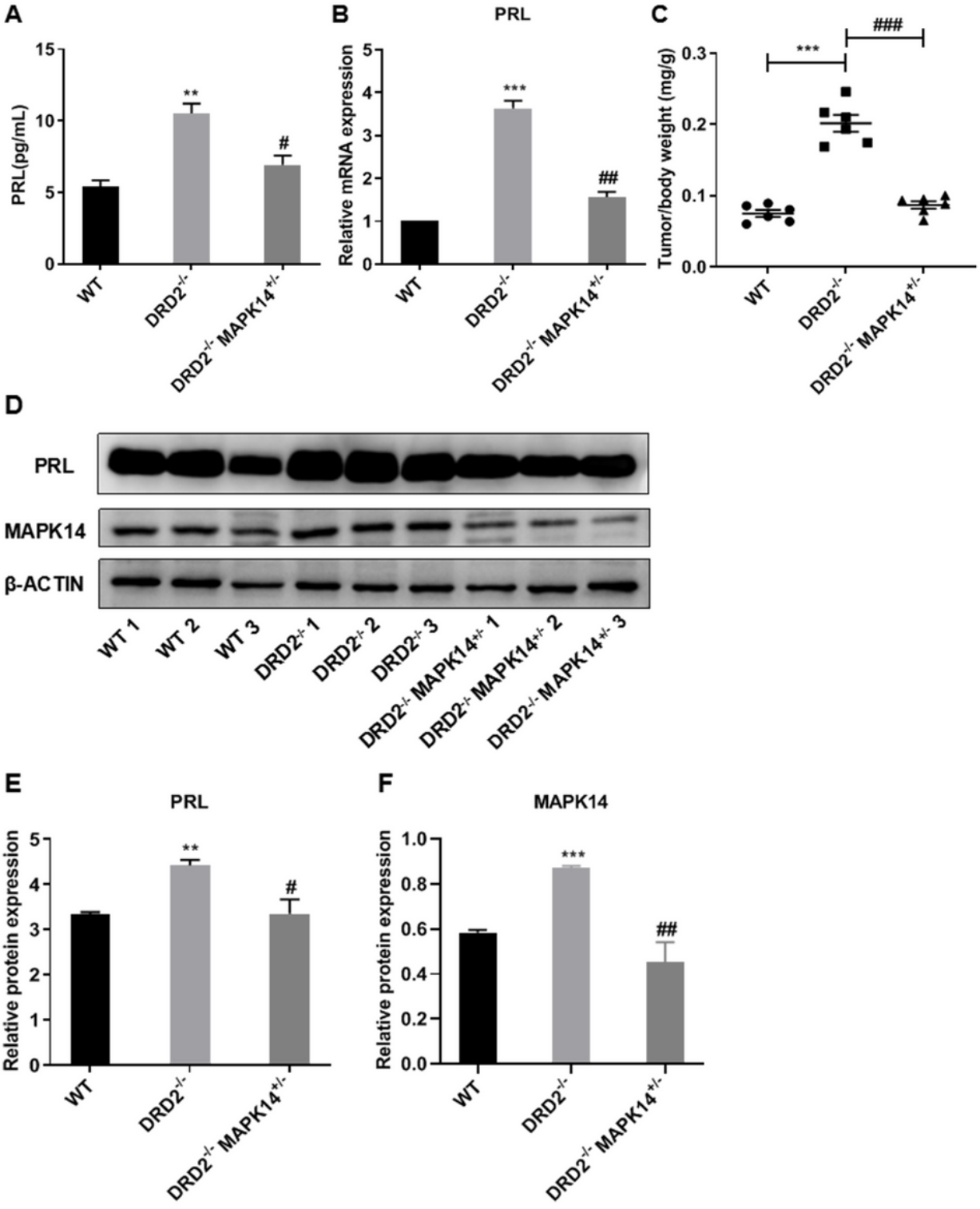

Figure 3

Effects of MAPK14 knockout on the development of prolactinomas in DRD2-/- mice. (A) Serum PRL level of wild-type (WT) mice, DRD2-/- mice and DRD2-/-MAPK14+/- mice by ELISA. **P<0.01 compared with WT mice group, #P<0.05 compared with DRD2-/- mice group, (n = 3). (B) The relative PRL mRNA

expressions of pituitary gland in mice were detected by RT-qPCR. ***P<0.001 compared with WT mice group, ##P<0.01 compared with DRD2-/- mice group, (n = 3). (C) The pituitary gland weight/body weight was calculated. ***P<0.001 compared with WT mice group, ###P<0.001 compared with DRD2-/- mice group, (n = 6). (D) The PRL protein expressions of pituitary gland in mice were detected by western blot. (E) The relative PRL protein expression was quantifed via normalization to β-actin. **P<0.01 compared with WT mice group, #P<0.05 compared with DRD2-/- mice group, (n = 3).

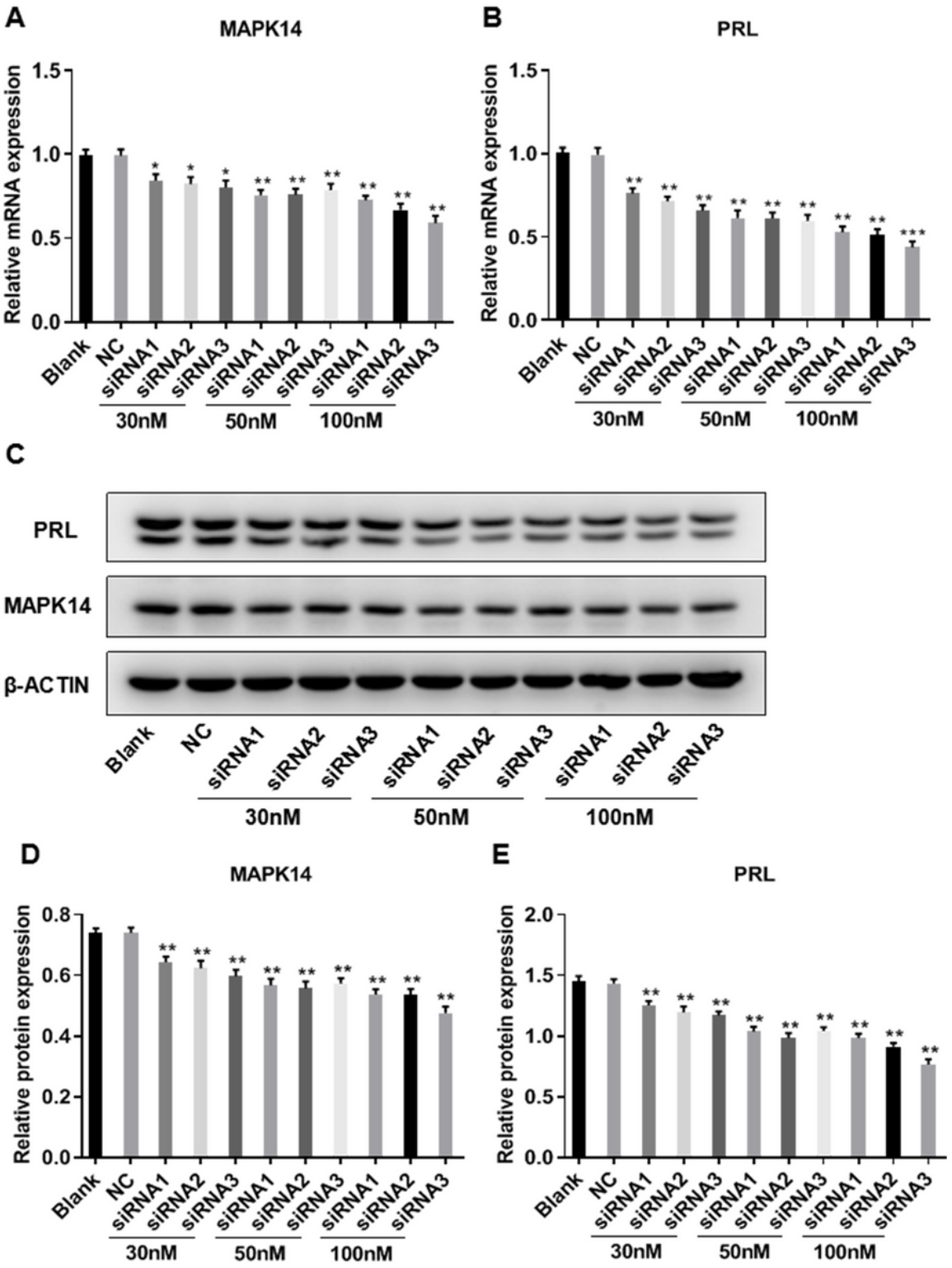

Figure 4

GH3 cells transfected with MAPK14 siRNA inhibited PRL production. (A) The effect of MAPK14 siRNA (30 nM, 50 nM, 100 nM) on MAPK14 in GH3 cells detected by RT-qPCR. *P<0.05 and **P<0.01 compared with NC group, (n = 3). (B) The effect of MAPK14 siRNA (30 nM, 50 nM, 100 nM) on PRL in GH3 cells detected by RT-qPCR. **P<0.01 and ***P<0.001 compared with NC group, (n = 3). (C) The effect of MAPK14 siRNA (30 nM, 50 nM, 100 nM) on MAPK14 and PRL in GH3 cells detected by western blot. (D, E) The relative protein expression of both MAPK14 and PRL were quantifed via normalization to β-actin. **P<0.01 compared with NC group, (n = 3).

Supplementary Files

This is a list of supplementary files associated with this preprint. Click to download.

- NC3RsARRIVEGuidelinesChecklistfillable.pdf